

Ground Behaviour Around a Tunnel Using Various Soil Models

Eshagh Namazi

Researcher, Department of Geotechnics and Transportation, Faculty of Civil Engineering, Universiti Teknologi Malaysia; email: eshagh.namazi@gmail.com

Hisham Mohamad

Senior Lecturer, Department of Geotechnics and Transportation, Faculty of Civil Engineering, Universiti Teknologi Malaysia; email: mhisham@utm.my

Ahmad Kueh Beng Hong

Senior Lecturer, Department of Structure and Materials, Faculty of Civil Engineering, Universiti Teknologi Malaysia; email: kbahmad@utm.my

Mohsen Hajihassani

Researcher, Department of Geotechnics and Transportation, Faculty of Civil Engineering, Universiti Teknologi Malaysia; email: mohsen_hajihassani@yahoo.com

Siti Norafida Jusoh

Researcher, Department of Geotechnics and Transportation, Faculty of Civil Engineering, Universiti Teknologi Malaysia; e-mail: snorafida@utm.my

Seyed Vahid Alavi Nezhad Khaili Abad

Researcher, Department of Geotechnics and Transportation, Faculty of Civil Engineering, Universiti Teknologi Malaysia; e-mail: v_alavi_59@yahoo.com

ABSTRACT

Finite Element (FE) analyses are used world widely in geotechnical engineering to obtain the soil displacement caused by tunnelling. The surface settlement induced by tunnelling predicted by FE is known to be wider and shallower than the field measurements particularly for stiff clays with high coefficient of earth pressure at rest, K_0 . It has been recognized that neglecting the non-linearity, anisotropy and three-dimensional effects of the soil model as well as K_0 condition can be the reasons of this discrepancy. Unfortunately, such numerical studies were only limited to the problem in the plane strain condition whereas tunnelling is obviously a three dimensional (3D) problem. This paper compares 3D FE modelling of tunnel constructions in stiff soil of London Clay using non-linear soil model with low and high K_0 regimes. It was found that modelling using isotropic non-linear soil with low value of K_0 gave the best matched-fit data on the observed greenfield surface settlement as opposed to the other soil models. In addition, the model is able to replicate the steady-state condition of ground movement after the completion of tunnel construction that is when the tunnel face has passed seven times of the tunnel diameter beyond the boundary point. This steady-state condition is not possible to simulate using other soil models.

KEYWORDS: Numerical modelling, settlement, non-linear, tunnel, excavation

INTRODUCTION

Accurate prediction of surface settlement induced by tunnelling in the urban area is an important duty for tunnel engineers to ensure that the adjacent buildings are adequately safe. Numerical analyses have been widely used for prediction of ground settlement. However, it is revealed that the surface settlement trough estimated using Finite Element (FE) method particularly in the stiff clays with high value of coefficient of lateral earth pressure at rest, K_0 , (e.g., London's clay) is much wider and shallower than the field data. Reasons for the discrepancy include the use of pre-failure soil model, K_0 conditions and simulation of three-dimensional effects of tunnel excavation (eg. Masin, 2009).

It was accepted by previous researchers (e.g., Gunn, 1993; Addenbrooke et al., 1997; Franzius et al., 2005) that numerical analyses incorporating the non-linear soil model with low- K_0 regime gives better surface settlement trough than the linear with high- K_0 regime. Only few studies directly compare the results of both models in 3D analyses. Addenbrooke et al. (1997) for instance presented a series of plane strain analysis, including linear elastic and non-linear elastic pre-yield models. They concluded that the non-linear model considerably gives the deeper and narrower surface settlement than linear model although their result was still shallower and wider than the measured data. Studies on the use of 3D numerical modelling include Masin (2009), Yazdchi et al. (2006), Dasari et al. (1996) and Franzius et al. (2005). Franzius et al. (2005) for example showed adopting soil anisotropy parameters derived from laborious experiments does not significantly improve the settlement profile in 3D FE modelling (Appendix A explains anisotropic soil model and its parameters). To improve the settlement trough, they adjusted fictitious soil anisotropy parameters for London Clay. Wongsaroj (2005) suggested a complex soil model considering non-linearity and anisotropy behaviour of the soil on the prediction regarding tunnel lining performance, generation of excess pore pressure and surface ground displacement. His soil model showed the narrowest surface settlement when compared with simple linear-elastic model. However the author's result was still wider than the Gaussian curve with $K_0=0.5$.

The aim of this study is to improve the surface settlement prediction by means of 3D numerical simulation using fairly simple nonlinear elastic-perfectly plastic soil model with stiffness $K_0=0.5$. The computed greenfield ground settlements are compared to the reported field measurements at St. James's Park, London together with analyses made by Franzius et al. (2005) of non-linear anisotropic soil models.

Description of the Site

The Jubilee Line Extension of London's subway consists of the westbound and eastbound twin tunnel's running through the South and East London. In this paper, the well documented of the westbound tunnel beneath St. James' Park is re-examined. The St. James' Park site is a green field site located between Westminster and Green Park Stations. The tunnel was excavated in London Clay using an open-face shield machine with tunnel diameter $D=4.75$ m and depth approximately $Z_0=30.5$ m. Further details of the site investigation and tunnelling method are given in Nyren (1998) and Standing and Burland (1999).

3D Numerical Analysis

The analyses presented in this paper were carried out using ABAQUS 6.10 Finite Element program. Reduced integration with full Newton solution technique and error-controlled sub

stepping stress point algorithm for solving the non-linear FE equations were adopted. The analyses were performed in the undrained conditions.

Geometry

Figure 1 shows the 3D FE mesh of the westbound tunnel. Only half of the problem was modelled since the geometry is symmetrical. The dimensions of the model were chosen to be identical with the model used by Franzius (2004), i.e. height 50m, length 150m and width 80m. To prevent the effects of far field boundary particularly on the longitudinal surface settlement, only 100 m out of 150 m model length is excavated (i.e. from $y=0.0$ m to $y=100.0$, see Figure 1). The soil mesh used in the analyses consists of 21,156 8-node hexagonal elements with 31,024 nodes. A hydrostatic pore water pressure distribution was defined based on water table 2 m below the ground surface. In all vertical sides of the model, normal horizontal displacement movements were restrained, whereas for the base of the mesh movements in all directions were restricted.

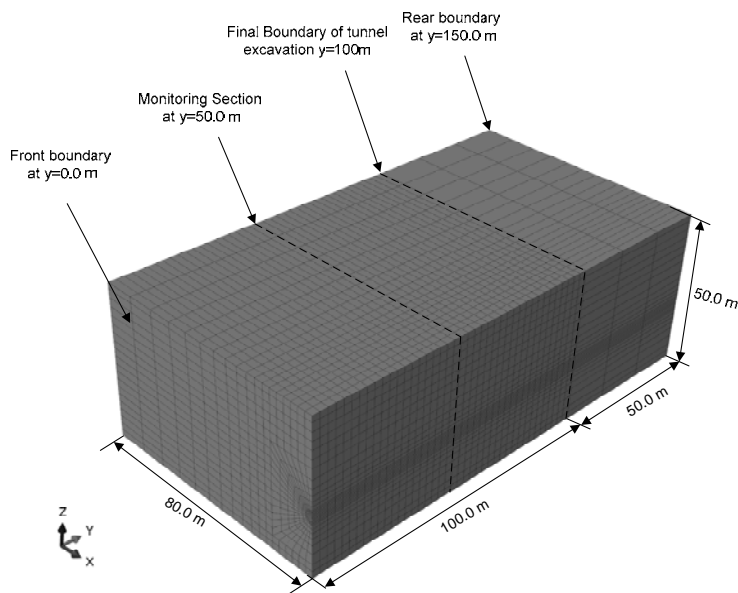


Figure 1: 3D Finite Element model of tunnel in ABAQUS

Simulation of Tunnel Construction

Figure 2 shows the sequence of tunnel construction consisting of excavation (deletion of soil elements inside the tunnel) and lining construction (activation of shell elements around the tunnel). The soil element is removed in a length equal to the excavation length L_{exc} and is left unsupported to allow ground deformation. The volume of surface settlement is calculated (also known as volume loss). The volume loss is calculated in the plane of the tunnel by dividing the volume of ground loss with the tunnel volume (Figure 3). After the volume loss has reached a specific value, the lining element is installed. The simulation of tunnel construction is continued by repeating in sequence between the soil elements removals and lining activation. A total of 40 steps were simulated for this model.

Example of two continuing steps where latest elements of slice 3 and 4 inside the tunnel are excavated is shown in Figure 2. The lining element is activated at one excavation length behind the tunnel face. Note that reducing the L_{exc} will obviously decrease the volume loss but increase the excavation steps. Adopting $L_{exc}=2.5$ m in this study (similar to one used by Franzius et al,

2005), the volume loss is measured as $VL = 3.8\%$ which is close to the $VL = 3.3\%$ observed in the field.

The tunnel lining was modelled by elastic shell element (Schroeder, 2003). The concrete lining was 0.168m thick and its Young's modulus and Poisson ratio were taken as 28 GPa and 0.15 respectively. The mesh tie constraints called "master-slaves" formulation were used to model the interaction between the lining and soil (ABAQUS, 2010). In modelling the interaction problem, the displacement and pore pressure of the "slaves" surface is made equal to value of the master surface to which it is the closest. In general, the master surface is a surface of stiffer body or coarser mesh, whereas the slave surface is a deformable body with finer mesh.

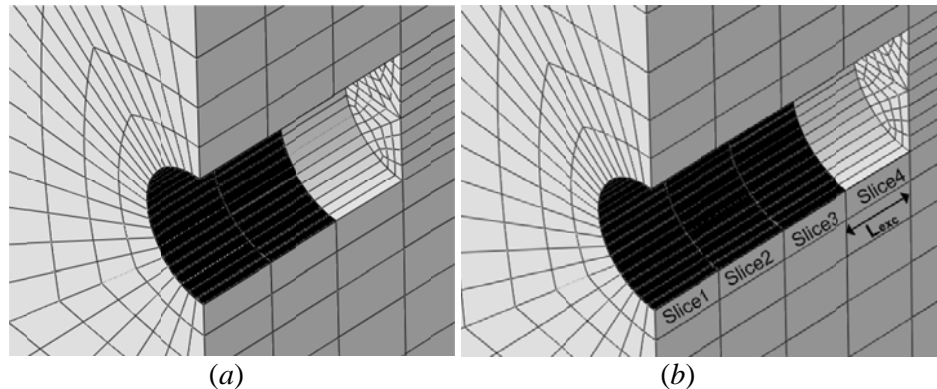


Figure 2: Simulation of tunnel construction in the two continuous steps: (a) Step 4 and (b) Step 5

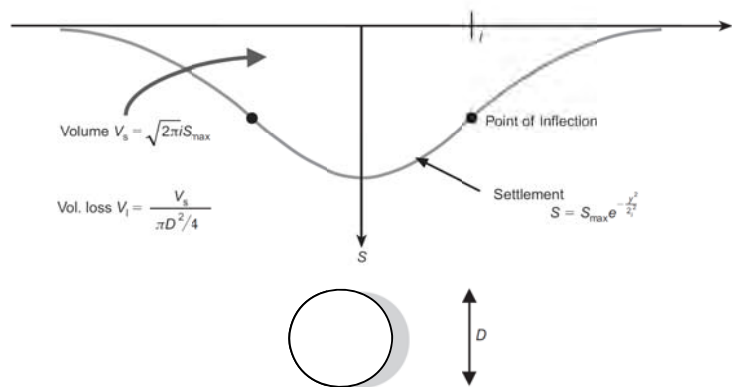


Figure 3: The Volume Loss definition

Constitutive Soil Models

The model of London Clay was described as elastic-perfectly plastic soil. In the plastic part (post yield), the Mohr-Coulomb yield surface was employed. The input parameters in this part are cohesion $c' = 5.0$ kPa, friction angle $\phi' = 25^\circ$ and dilation angle $\psi' = 12.5^\circ$. The elastic part (pre-yield) was expressed as isotropic non-linear elastic behaviours which are explained in the next section.

Pre-yield soil behaviour

Isotropic non-linear soil model

Using local strain measurements on triaxial samples (Burland & Symes, 1982), it was found that the behaviour of London Clay at small strains is highly non-linear. Figure 4 shows the non-linearity when plotting the normalized undrained soil stiffness E_u versus axial strain ϵ_{ax} . Because the undrained strength in the laboratory is depended on many factors, Jardine et al. (1986) preferred the normalization against mean effective stress P' . The following expression for tangent shear and bulk modulus are used in this numerical analysis.

$$\frac{G}{p'} = A + B \cos(\alpha X^\gamma) - \frac{B\alpha\gamma X^{\gamma-1}}{2.303} \sin(\alpha X^\gamma) \quad (1)$$

$$\frac{K'}{p'} = R + S \cos(\delta Y^\eta) - \frac{S\delta\eta Y^{\eta-1}}{2.303} \sin(\delta Y^\eta) \quad (2)$$

where,

$$X = \log_{10}\left(\frac{E_d}{\sqrt{3}C}\right)$$

$$\delta = \log_{10}\left(\frac{|\epsilon_v|}{T}\right)$$

G is secant shear modulus, K secant bulk modulus, P' mean effective stress, E_d and ϵ_v deviatoric and volumetric strain variants and constant A , B , R , S , α , δ , γ , η are given in Table 1 for London Clay.

The above equations only hold for a specific range of strain values. For strains below a lower limit ϵ_{\min} and above an upper limit ϵ_{\max} , fixed tangent stiffness's are assumed. In the undrained isotropic conditions with Poisson's ratio of 0.49, the undrained Young's modulus $E_u=3G$ and $\epsilon_v=0$. From Equations 1 and 2 the Young's modulus is

$$\frac{E_u}{p'} = A + B \cos\left\{\alpha\left(\log_{10}\left(\frac{E_d}{\sqrt{3}C}\right)\right)^\gamma\right\} \quad (3)$$

To implement this form of non-linearity into ABAQUS software, the author has written a subroutine for the constitutive model. The "USDFLD" subroutine was used to include user-defined field variables of deviator strain and mean effective stress in definition of material properties.

Table 1: Pre-yield input parameter in London Clay (after Jardine *et al.* 1986)

A	B	C	α	γ	Ed(min)	Ed(max)	Gmin(kPa)
1120	1016	0.0001	1.335	0.617	8.660253*10 ⁻⁴	0.692820	2333.3
R	S	T	δ	η	ϵ_v (min)	ϵ_v (max)	Kmin(kPa)
549	506	1.03*10 ⁻³	2.069	0.420	5.03*10 ⁻³	0.15	3000

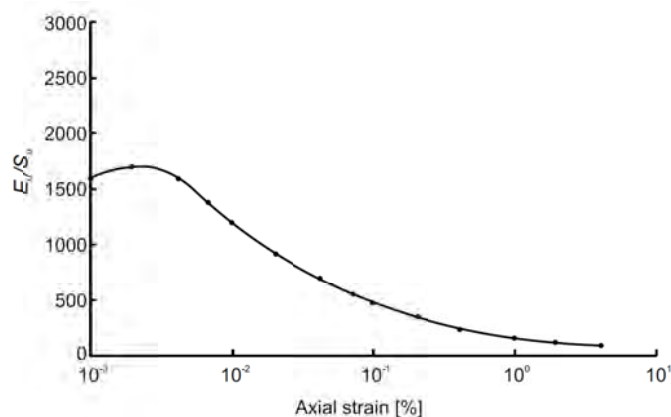


Figure 4: Typical Stiffness-strain characteristics of London Clay. (After Mair, 1993)

Initial Conditions

Before the tunnelling process is modelled, the initial conditions which are affected by the geological history of the site must be applied. In ABAQUS, initial conditions are achieved by specifying the distribution of vertical and horizontal geostatic effective stresses, pore water pressure, void ratio and saturation in the whole depth of soil. The vertical effective stress caused by soil weight was specified based on elevation-dependent initial stress. It means that the vertical stress is varying linearly with vertical coordinate. The saturated bulk unit weight of the soil is assumed 20 kN/m^3 .

The horizontal effective stress, σ_{11} at a point was specified by entering the “coefficient of lateral earth pressure at rest”, K_0 which defines the lateral components of effective stress as the vertical stress, σ_{33} at the point multiplied by the value of the coefficient. The coefficient of earth pressure at rest for London Clay varies with depth and it ranges between 0.75 and 2.3 at the top, and between 1 and 2 at approximately 35 m below the ground surface (Nyren, 1998). It was illustrated by Addenbrooke et al. (1997) and Franzius et al. (2005) that the simplification of choosing the average value of $K_0=1.5$ is unlikely to have a major influence on the results. However, selection of high K_0 value of 1.5 gives greater mean effective stress and soil stiffness consequently (see Equation 3). Modelling the tunnel in the soil with high stiffness obtains smaller ground displacement. To achieve an improved prediction of surface settlement above a greenfield-tunnel excavation, fictitious soil stiffness with low K_0 value model is proposed.

Analysis Results

Effects of initial K_0 on the coefficient of lateral effective stress

Figures 5 and 6 illustrate the changes of effective horizontal and vertical stresses across the points of around the tunnel ring (measured from crown to invert) in the monitoring section ($y=50 \text{ m}$) when $K_0=1.5$ and $K_0=0.5$ respectively. These figures show the stresses for three stages of the modelling: prior to any tunnel excavation, when the tunnel face is under the monitoring section ($y=50 \text{ m}$) and after the end of tunnel excavation ($y=100 \text{ m}$). Prior to tunnel excavation, the soil is under geostatic condition and effective stresses vary linearly with vertical coordinate. The excavation changes the stress distribution in all locations around the tunnel. In the case of initial $K_0=1.5$, the vertical stress, σ_{33} (Figure 5b) increased at all points with maximum value at tunnel springline, whereas the horizontal stress, σ_{11} (Figure 5a) at the springlines decreased to the

minimum value. In contrast, when the initial condition is based on $K_0=0.5$, the horizontal effective stress increased at all points around the tunnel with maximum in crown and invert but vertical stress decline slightly at the springlines.

The coefficient of lateral effective stress, K_{13} is defined as the ratio of horizontal effective stress, σ_{11} to the vertical effective stress, σ_{33} (the K_0 was the ratio σ_{11}/σ_{33} under the zero lateral tensile strain condition). Figure 7 shows the changes of coefficient of lateral stress $K_{13}(=\sigma_{11}/\sigma_{33})$ before and after tunnel construction when modelling using $K_0=0.5$ and 1.5. In the case of $K_0=1.5$, the coefficient K_{13} increased to 1.8 at the crown and invert but decreased to around 0.6 at the springlines. Conversely, the simulation with low-value of $K_0=0.5$ resulted in an increase of the stress coefficient to 1.6 at the invert and crown but remain constant at the tunnel springline. Interestingly, the figure illustrates that even varying the K_0 from 1.5 to 0.5, the final distribution of K_{13} around the tunnel is about the same for both cases and only differs to about 10% in terms of its ratio.

It is clear that the coefficient of lateral effective stress, K_{13} increases with decreasing the vertical stress and decreases with decreasing the horizontal stress. Excavation of the tunnel causes relaxation of vertical stress at the crown and invert of the tunnel whereas at the springlines, the horizontal stress reduction is more significant. Further study is currently undertaken to quantify the effect of K_0 to the three dimensional behaviour of tunnel lining and stress changes ahead of the tunnel face as well as mapping the suitable initial K_0 regime when modelling tunnel construction in plain-strain condition.

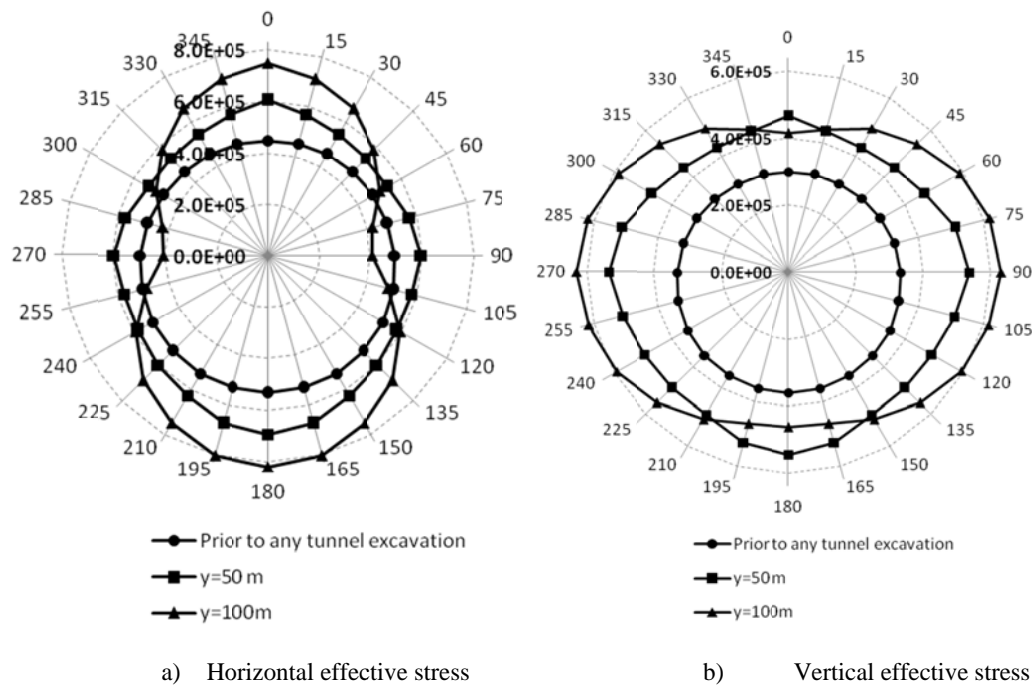


Figure 5: Effective stresses around the tunnel in the monitoring section for different excavation stages when $K_0=1.5$

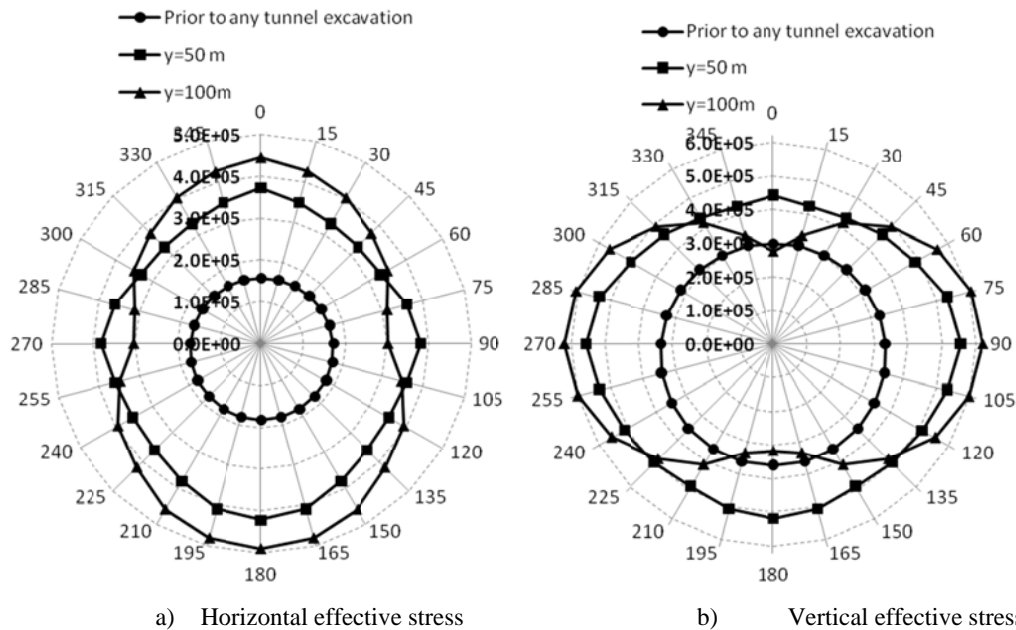


Figure 6: Effective stresses around the tunnel in the monitoring section for different excavation stages when $K_0=0.5$

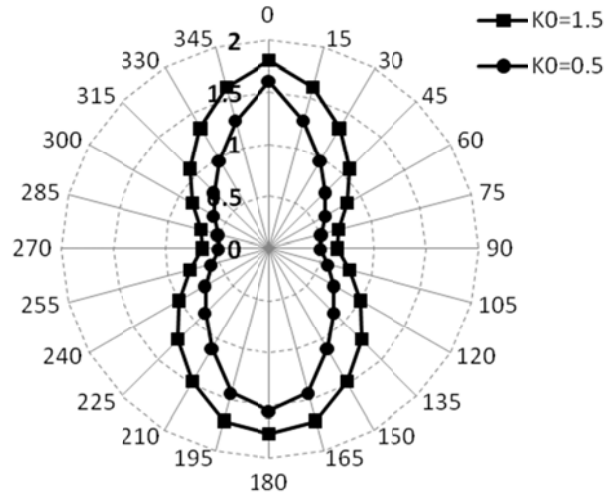


Figure 7: The Coefficient of lateral stress, K_{13} after excavation of the tunnel for different initial K_0

Transverse Surface Settlement at St James' Park Tunnel

This section investigates the difference tunnel-induced surface settlement troughs for isotropic and anisotropic soils with varying K_0 . The analyses presented here are compared with field data by Nyren (1998), 3D FE by Franzius *et al.* (2005) of similar soil properties, construction sequence (e.g. excavation length) and tunnel geometry. The London Clay was

modelled as transversely anisotropic by Franzius *et al.* (2005) whereas this study adopts isotropic non-linear elastic and Mohr-Coulomb plastic with $K_0=1.5$ and $K_0=0$.

Figure 8 shows two sets of transverse settlement profiles at two different construction times. Figure 8a presents settlement in the monitoring section when the tunnel face was exactly beneath the monitoring section ($y=50$ m) which is referred by Nyren (1998) as data Set 22. The monitoring sections of the model are shown in Figure 1. Figure 8b shows the surface settlement at monitoring section when the tunnel face passed 50 m away from the monitoring section (i.e. $y=100$ m). The field data by Nyren (1998) in Figure 8b is referred to as Set 29. As Nyren (1998) reported no further short-term settlement after this set, this measurement can be taken as the end of immediate settlement response.

Figure 8a compares isotropic cases with $K_0=0.5$ and $K_0=1.5$ with field data. For $K_0=1.5$, the surface settlement trough is shallower and too wide when compared to the field data. The maximum surface settlement of 5.4 mm was obtained in the isotropic soil with initial high-value of $K_0=1.5$ whereas the true maximum settlement was actually 12 mm. Conversely in the case of $K_0=0.5$, the present study indicated a maximum surface settlement trough similar to the field data. However, as any Finite Element analyses, the shape of the settlement trough can still considered to be wider than the field data.

Similar trends are also observed in Figure 8b where the isotropic $K_0=1.5$ showed a very shallow and wide trough compared to the field data with volume loss V_L of only 2.1%. A high degree of anisotropic soil model (parameter "Set 2" in Table 2) with low $K_0=0.5$ by Franzius *et al.*, (2005) also did not match well with the observed field data. The surface settlement calculated from the anisotropic soil model was as much as 86 mm compared to the actual 20.5 mm, leaving a significant high value of volume loss V_L of 18.1%. Franzius *et al.*, (2005) illustrated little improvement in the transverse trough when a level of anisotropy appropriate for London clay (Data "set 1" in Table 2) was adopted. On the other hand, the much simpler soil model based on isotropic with $K_0=0.5$ used in this study matched fairly well with the observed field measurement. The volume loss in this case is $V_L=3.8\%$ which is near to $V_L=3.3\%$ observed in the field measurement.

It is important to note that all the 3D numerical analyses presented here were performed with same excavation length of L_{exc} . It can be seen from Figure 8 that the isotropic soil model with $K_0=0.5$ gave the best results of all the three types of pre-yield soil models. The findings enable the authors to continue selecting this model for the subsequent analyses in investigating the effects of tunnel excavation underneath existing building.

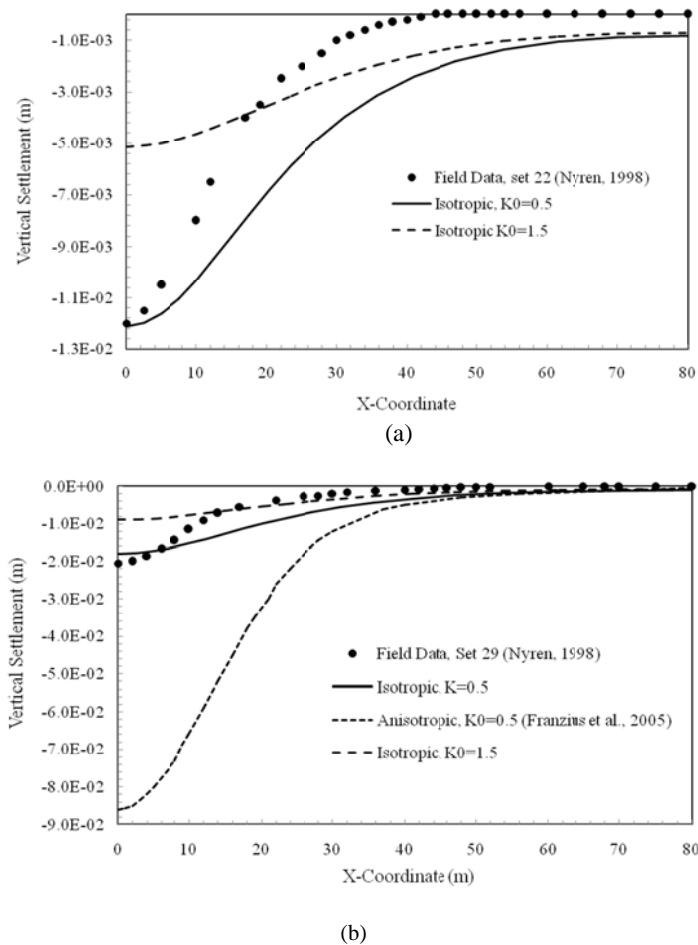


Figure 8: Transverse surface settlement from 3D analyses and field measurement for St. James' Park tunnel

Longitudinal Settlement Profiles From Isotropic Soil Model in $K_0=0.5$

In this section, the development of surface settlement profiles in isotropic soil with high and low K_0 -regimes are investigated in order to establish at which stage the steady-state condition develops. The steady-state is defined as the point at which the settlement does not change with continuing tunnel construction. The criterion for steady-state condition of surface settlement is an important subject particularly when analysing performance of buildings subjected to tunnelling induced ground movements.

Figure 9 generally shows longitudinal settlement profile along the model for different excavation stages (arrows indicating position of tunnel face). The figure shows that during the first few excavation steps, the shape of longitudinal settlement is similar to cumulative error curve but as the tunnel construction progresses, the shape of settlement changes slightly with

development of “hogging” deformation at the tunnel’s tail. This may be related to the boundary effect of the FE model.

Figure 9a illustrates that steady-state condition is not established during the 3D analyses with isotropic soil model when $K_0=1.5$. Additional settlement at the front boundary ($y=0$ m) can still be seen although the tunnel face has reached the final excavation step at $y=100$ m. This means larger FE model is needed to allow longer tunnel construction and achieve the steady-state condition at the front boundary.

Figure 9b presents the development of surface settlement in the isotropic soil with $K_0=0.5$. In contrast to the previous figure, Figure 9b shows the front boundary settlement does not change significantly when tunnel face passed approximately $y=30$ m away. Figure 10 shows a much clearer description in defining when surface settlement has reached the steady-state condition. It can be seen in this figure that surface settlement increment at the front boundary is very minimal approximately when tunnel face has reached $y= 30$ m. This can be referred as the steady-state condition.

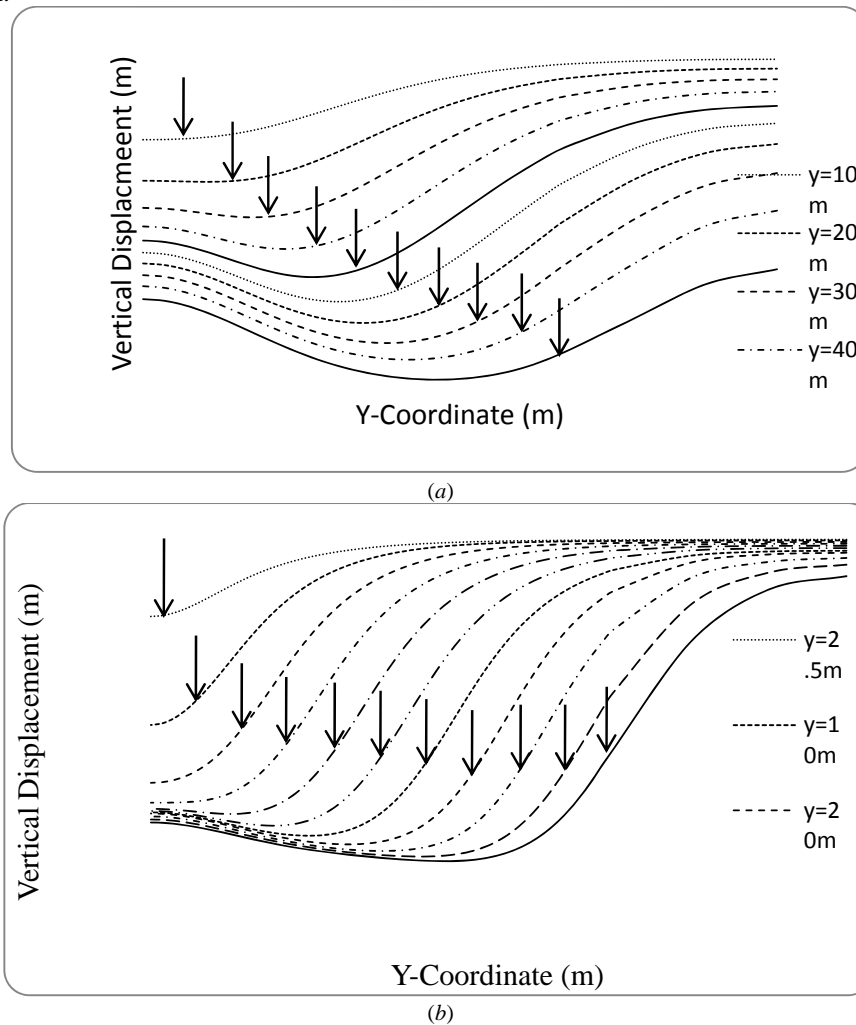


Figure 9: Longitudinal Surface Settlement in initial (a) $K_0=1.5$ and (b) $K_0=0.5$

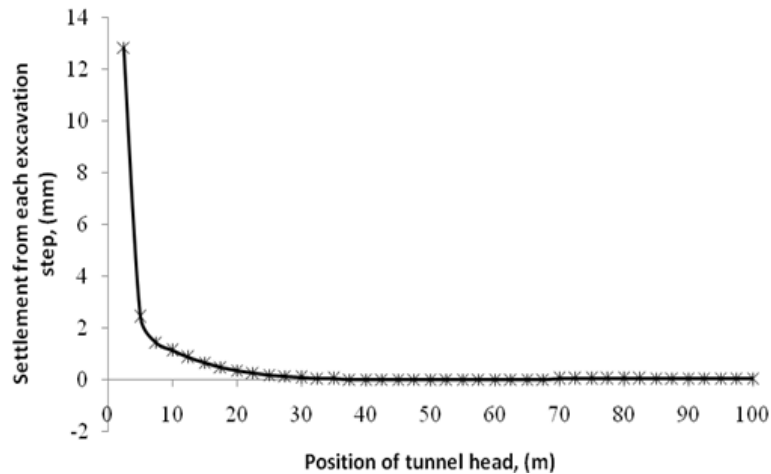


Figure 10: Incremental surface settlement during the progress of tunnel excavation measured above tunnel centreline at the front FE boundary

CONCLUSION

In this study, 3D numerical analyses of tunnelling in London Clay were performed using isotropic non-linear soil model with different K_0 regime. It was shown that the coefficient of lateral stress K_{13} ($=\sigma_{11}/\sigma_{33}$) for initial values of $K_0=1.5$ increased to 1.8 at crown and invert of the tunnel and decreases to around 0.6 at springline after excavation of the tunnel. In contrast K_{13} for initial values of $K_0=0.5$ remained constant at the springline. The final distribution of K_{13} ratio around the tunnel lining for both initial conditions however is almost similar.

The study also indicated that coefficient of the earth pressure at rest, K_0 significantly affects the surface settlement trough. The comparison of settlement profile with field measurement of London Clay obtained from St. James' Park case study showed that the non-linear soil with low- K_0 regime gave better settlement profile compared to anisotropic soil model of high initial K_0 regime.

The longitudinal surface settlement profile caused by the tunnelling using non-linear soil model with $K_0=0.5$ was able to produce the steady-state condition. This was achieved when the tunnel face was seven times of tunnel diameter away from the front boundary or $y=30$ m. Decreasing the K_0 value of soil enables the model to achieve the steady-state conditions at an earlier stage of tunnel construction. This is important if one requires analysing building performance to tunnel induced ground movement.

REFERENCES

1. Abaqus6.10. (2010). "User's manual". Hibbit, Karlson and Sorenson, Inc.
2. Addenbrooke, T., Potts, D., and Puzrin, A. (1997). "The influence of pre-failure soil stiffness on the numerical analysis of tunnel construction"., *Geotechnique*, 47(3), 693–712.
3. Burland, J.B., Symes, M. (1982). "A simple axial displacement gauge for use in the triaxial apparatus". *Geotechnique*, 32(1), 62-65.

4. Dasari, G.R., Rawlings, C.G., and Bolton, M.D. (1996). "Numerical modeling of a NATM tunnel construction in London clay". In *Proceedings of the 1st International Symposium on the Geotechnical Aspects of Underground Construction in Soft Ground*, London, U.K., 15–17 April 1996. Edited by R.J. Mair and R.N. Taylor. A.A. Balkema, Rotterdam, The Netherlands. pp. 491–496.
5. Franzius, J. N. (2004). "Behaviour of building due to tunnel induced subsidence". *Ph.D. thesis*. Imperial College of Science, Technology and Medicine, London.
6. Franzius, J. N., Potts, D. M., and Burland, J. B. (2005). "The influence of soil anisotropy and K_0 on ground surface movements resulting from tunnel excavation". *Géotechnique*, 55(3), 189–199.
7. Grammatikopoulou, A., John, H. D., St, Potts, D. M. (2008). "Non-linear and linear models in design of retaining walls". *Geotechnical Engineering* 161(GE6), 311–323.
8. Graham, J. and Houlsby, G.T. (1983). "Anisotropic elasticity of natural clay". *Géotechnique*, 33(2), 165-180.
9. Gunn, M. J. (1993). "The prediction of surface settlement profiles due to tunnelling". *Proc., Worth Memorial Symp.*, Thomas Telford, London, 304–316.
10. Jardine, R.J., Potts, D.M., Fourie, A.B. and Burland, J.B. (1986). "Studies of the influence of non-linear stress-strain characteristic in soil-structure interaction". *Géotechnique*, 36(3), 377-396.
11. Mair, R. J. (1993). The Unwin Memorial Lecture 1992: "Developments in geotechnical engineering research: application to tunnels and deep excavations". *Proc. Instn. Civ. Engrs. Civil Engineering*, 97, 27-41.
12. Masin, D. (2009). "3D modeling of an NATM tunnel in high K_0 clay using two different constitutive models". *Journal of Geotechnical and Geoenvironmental Engineering*, 135(9), 1326-1335.
13. Nyren, R. (1998). "Field measurement above twin tunnel in London Clay". *PhD thesis*, Imperial College, University of London.
14. Schroeder, F.C.(2003). "The influence of bored piles on existing tunnels". *Ph.D. thesis*, Imperial College, University of London.
15. Standing, J.R. and Burland, J.B. (1999). "Report on ground characterisation to explain tunnelling volume losses in the Westminster area". *Internal report, Imperial College of Science Technology and Medicine*.
16. Wongsaroj, J. (2005). "Three-dimensional finite element analysis of short and long-term ground response to open-face tunnelling in stiff clay". *Ph.D. Thesis*, University of Cambridge.
17. Yazdchi, M, Macklin, S. R, and Yeow, H. C. (2006). "3D modelling of sprayed-concrete-lined tunnels in clay, *Geotechnical Engineering*". *Proc. Inst Civ. Eng. (Lond.)*, Vol. 159(Issue 4): 243–250.

Appendix A: Anisotropic non-linear soil model

An updated form of transverse anisotropic stiffness with non-linear stiffness behaviour of the soil is used by many authors to study the effects of anisotropy on the ground movement (*e.g.* Addenbrooke *et al.*, 1997; Franzius *et al.* 2005; Grammatikopoulou *et al.*, 2008). The soil model is described by three

independent material parameters namely the vertical Young's modulus, E_v , the Poisson's ratio for horizontal strain due to horizontal strain in the orthogonal direction, ν_{hh} and an anisotropic scale parameter α which is defined as following:

$$\alpha = \sqrt{\frac{E_h}{E_v}} = \frac{\nu_{hh}}{\nu_{vh}} = \frac{G_{hh}}{G_{vh}} \quad (4)$$

where E_h is the horizontal Young's modulus, ν_{vh} is the Poisson's ratio for horizontal strain due to vertical strain, G_{hh} is the shear modulus in the horizontal plane and G_{vh} the shear modulus in the vertical plane. In the isotropic cases, the parameter of anisotropy is $\alpha=1$. The tangent vertical Young's modulus E'_v is expressed as (Graham and Houlsby, 1983):

$$\frac{E'_v}{p'} = A_\alpha + B_\alpha \cos(\beta X^\gamma) - \frac{B_\alpha \beta \gamma X^{\gamma-1}}{6.909} \sin(\beta X^\gamma) \quad (5)$$

Two parameter sets, refers to "Set 1" and "Set 2" adopted by Franzius *et al.* (2005) are summarized in Table 2. The first set represents a degree of anisotropy that is suitable for London Clay and the second set incorporates an extremely high degree of anisotropy which is more academic interest and does not supported by any literature.

Table 2: Parameters for anisotropic pre-yield model (Franzius *et al.*, 2005)

Parameter "Set 1" appropriate for London Clay obtained from field data									
A_α	B_α	C	β	γ	$E_{d, \min}:\%$	$E_{d, \max}:\%$	$E_{v, \min}:\text{kPa}$	α	ν_{hh}'
373.3	338.7	1×10^{-4}	1.335	0.617	8.66×10^{-4}	0.69282	5558.8	1.265	0.4
Parameter "set 2" incorporate fictive high degree of anisotropy α									
308.8	280.2	1×10^{-4}	1.335	0.617	8.66×10^{-4}	0.69282	5558.8	2.5	0.1

